

On a regularization of the compressible Euler equations for an isothermal gas

H. S. Bhat* R. C. Fetecau†

February 5, 2009

Abstract

We consider a Leray-type regularization of the compressible Euler equations for an isothermal gas. The regularized system depends on a small parameter $\alpha > 0$. Using Riemann invariants, we prove the existence of smooth solutions for the regularized system for every $\alpha > 0$. The regularization mechanism is a nonlinear bending of characteristics that prevents their finite-time crossing. We prove that, in the $\alpha \rightarrow 0$ limit, the regularized solutions converge strongly. However, based on our analysis and numerical simulations, the limit is not the unique entropy solution of the Euler equations. The numerical method used to support this claim is derived from the Riemann invariants for the regularized system. This method is guaranteed to preserve the monotonicity of characteristics.

1 Introduction

We begin with the compressible Euler equations for an isothermal gas in one spatial dimension:

$$\rho_t + (\rho v)_x = 0, \tag{1a}$$

$$v_t + vv_x + \kappa \frac{\rho_x}{\rho} = 0. \tag{1b}$$

Here ρ denotes the mass density and v the velocity of the gas. The constant κ is taken to be positive. Subscripts denote partial differentiation. One obtains (1) from the compressible Euler system by choosing the pressure function $p(\rho) = \kappa\rho$. Then $c = \sqrt{p'(\rho)} = \sqrt{\kappa}$ is the sound speed. The system may be written in the form

$$\begin{pmatrix} \rho \\ v \end{pmatrix}_t + A_0 \begin{pmatrix} \rho \\ v \end{pmatrix}_x = 0, \tag{2a}$$

$$A_0 = \begin{pmatrix} v & \rho \\ \kappa/\rho & v \end{pmatrix}. \tag{2b}$$

*School of Natural Sciences, University of California, Merced, P.O. Box 2039, Merced, CA 95344, USA (hbhat@ucmerced.edu)

†Department of Mathematics, Simon Fraser University, Burnaby, BC V5A 1S6, Canada (van@math.sfu.ca)

The following facts are well-known: system (2) has the Riemann invariants $w_1 = v + \sqrt{\kappa} \log \rho$ and $w_2 = v - \sqrt{\kappa} \log \rho$. These Riemann invariants are used to show that if there exists x_0 such that either $w_{1,x}(x_0, 0) < 0$ or $w_{2,x}(x_0, 0) < 0$, then the solution of (2) with smooth initial data must develop a discontinuity in finite time. In other words, for a large set of smooth initial data, system (2) fails to have classical solutions that exist for all $t \geq 0$.

In the present work, we consider a system where the diagonal elements of the A_0 matrix (2b) have been smoothed. That is, we fix the constant $\alpha > 0$ and consider the system

$$\begin{pmatrix} \rho \\ v \end{pmatrix}_t + A \begin{pmatrix} \rho \\ v \end{pmatrix}_x = 0, \quad (3a)$$

$$A = \begin{pmatrix} u & \rho \\ \kappa/\rho & u \end{pmatrix}, \quad (3b)$$

$$v = u - \alpha^2 u_{xx}. \quad (3c)$$

If $\alpha = 0$, then $u = v$, $A = A_0$, and system (3) reduces to system (2).

For $\alpha > 0$, the effect of the elliptic equation (3c) is to generate from v a smoothed or filtered velocity u . This can be easily seen in Fourier space. Using hats to denote Fourier transforms and letting q be Fourier conjugate to x , it is clear that (3c) is equivalent to $\hat{u} = \hat{v}/(1 + \alpha^2 q^2)$. For small $\alpha > 0$, the interpretation is that u is a low-pass filtered version of v . To our knowledge, the first person to suggest filtering the convective velocity in a fluid-dynamical equation was J. Leray [Ler34], so we refer to (3) as the Leray-Euler system.

There are three main results in this paper. First, for any $\alpha > 0$, and for initial data in the Sobolev space $W^{2,1}(\mathbb{R})$, the Leray-Euler system (3) is well-posed. Solutions (ρ, v) exist for all $t \geq 0$ and retain their initial smoothness. Second, a subsequence of the solutions (ρ^α, v^α) of (3) converges strongly as $\alpha \rightarrow 0$ to functions (ρ, v) that satisfy the velocity equation (1b) in the distributional sense. Third, using the characteristic form of (3), we develop a monotonicity-preserving numerical method that provides evidence that as $\alpha \rightarrow 0$, solutions of the Leray-Euler system (3) do not converge to the weak entropy solution of the Euler system (1).

Note that the proof of well-posedness for (3) uses the same Riemann invariants used to show classical ill-posedness of (2). Associated to the Riemann invariants are characteristic curves. As we will show, using the smoothed velocity field u on the diagonal of the A matrix (3b) has the effect of bending the characteristics and hence preventing them from crossing in finite time. We employed similar ideas in our previous and current work on the Leray regularization technique applied to the Burgers equation¹ [BF06, BF08, BF09].

We find remarkable the applicability of Riemann invariant/characteristic methods to the Leray-Euler system. To explain this further, note that the finite-time breakdown of classical solutions of (1) is often remedied by the addition of viscous or dissipative terms. When such parabolic terms are included, one no longer gains useful information from characteristics or Riemann invariants. To see the specific terms that distinguish the Leray-Euler system (3), we may substitute (3b) and (3c) into (3a). This gives

$$\rho_t + (\rho u)_x - \alpha^2 \rho u_{xxx} = 0, \quad (4a)$$

$$u_t + uu_x + \kappa \frac{\rho_x}{\rho} - \alpha^2 u_{txx} - \alpha^2 uu_{xxx} = 0. \quad (4b)$$

¹By the Burgers equation, we mean the inviscid equation $v_t + vv_x = 0$.

Again, choosing $\alpha = 0$ gives the Euler system (1). The extra $O(\alpha^2)$ terms all contain third-order derivatives; two are nonlinear and one has a mixed derivative in space and time. It is not obvious looking at these terms that they would stop the finite-time breakdown of classical solutions of (1). As we show, the classical technique of Riemann invariants can be used to establish global well-posedness for a system that can be viewed either as a coupled hyperbolic-elliptic system with no added dissipation, as in (3), or as a third-order nonlinear 2×2 system, as in (4). It remains to be seen whether these classical ideas can be applied to other nonlinear systems of a similar form.

As already noted, the motivation to study the Leray-Euler system (3) stems from our past work on the Leray-Burgers equation [BF06]. There it was proven that the Leray smoothing mechanism regularizes the Burgers equation and captures, as $\alpha \rightarrow 0$, a weak solution of the Burgers equation. Numerical evidence supported our conjecture that this weak solution was indeed the unique entropy solution. Additional work on the stability of traveling waves [BF08] and on the solution of Riemann problems [BF09] has confirmed that the Leray-Burgers equation mirrors the physics of shocks and rarefaction in the Burgers equation.

Further motivation was provided by our past study [BaJG07] of a Leray-type regularization for the isentropic Euler equation with a γ -law pressure function, $p(\rho) = \kappa\rho^\gamma$ ($\kappa, \gamma > 0$). There, using the asymptotic method of weakly nonlinear geometric optics [HK83, MR84], the authors concluded that the Leray regularization did not prevent finite-time blowup for $\gamma \neq 1$.

To our knowledge, the present work is the first to study a globally well-posed Leray regularization for any compressible Euler system, in one space dimension or otherwise.

2 Well-posedness of the initial value problem

In this section we study the existence, uniqueness and regularity of solutions of the Cauchy problem for the Leray-Euler system (3). Therefore we consider (3) with initial data

$$\rho(x, 0) = \rho_0(x), \quad v(x, 0) = v_0(x). \quad (5)$$

We use $\mathcal{H} = 1 - \alpha^2 \partial_{xx}$ to denote the Helmholtz operator so that $v = \mathcal{H}u$ is equivalent to (3c). Using the Green's function G^α of \mathcal{H} , we have an explicit formula for u in terms of v :

$$G^\alpha(x) = \frac{1}{2\alpha} \exp(-|x|/\alpha) \quad (6)$$

$$u(x, t) = G^\alpha * v := \frac{1}{2\alpha} \int_{\mathbb{R}} \exp(-|x - y|/\alpha) v(y, t) dy. \quad (7)$$

Riemann invariants. We first construct the Riemann invariants corresponding to the system (3). The matrix A defined by (3b) has eigenvalues $\lambda_1 = u - c$ and $\lambda_2 = u + c$, where $c = \sqrt{\kappa}$. The corresponding eigenvectors are $\mathbf{r}_1 = (\rho, -c)^T$ and $\mathbf{r}_2 = (\rho, c)^T$. Define w_1 and w_2 as

$$w_1(\rho, v) = v + \sqrt{\kappa} \log \rho, \quad (8a)$$

$$w_2(\rho, v) = v - \sqrt{\kappa} \log \rho. \quad (8b)$$

The two functions w_1 and w_2 satisfy $\nabla w_i(\rho, v) \cdot \mathbf{r}_i = 0$ for $i = 1, 2$. The \cdot represents the scalar product in \mathbb{R}^2 . We call w_1 and w_2 the Riemann invariants of the Leray-Euler system (3), by

analogy with the well-known definition of Riemann invariants for systems of conservation laws (see, for example, [Smo83]). If we take $v = u$ to reduce (3) to the Euler system (1), then w_1 and w_2 given by (8) are the classical Riemann invariants for (1).

By differentiating w_i with respect to t and x and using (3), one obtains:

$$w_{1,t} + \lambda_2 w_{1,x} = 0, \quad (9a)$$

$$w_{2,t} + \lambda_1 w_{2,x} = 0. \quad (9b)$$

This is a remarkable property of Riemann invariants: the i -Riemann invariant is constant along the j -characteristics ($i \neq j$). More precisely, define the two families of trajectories

$$\frac{d}{dt} \eta_i(X, t) = \lambda_j(\eta_i(X, t), t), \quad i, j = 1, 2 \text{ and } i \neq j, \quad (10)$$

subject to $\eta_i(X, 0) = X$, $i = 1, 2$. Here, X denotes the Lagrangian coordinate (particle label). Then it is clear that, as long as a smooth solution (w_1, w_2) of (9) exists, we have $\frac{d}{dt}[w_i(\eta_i(X, t), t)] = 0$, $i = 1, 2$. This implies

$$w_i(\eta_i(X, t), t) = w_i(X, 0), \quad t > 0, \quad i = 1, 2. \quad (11)$$

Of course, system (9) can be considered equivalent to system (3) (or (4)) only for smooth solutions. We will show below that system (9) admits classical solutions, provided the initial data is smooth enough. Then we infer a result regarding the existence of classical solutions for system (3).

The equations (9a) and (9b) for w_1 and w_2 are in ‘‘characteristic’’ form. Non-crossing of characteristics is equivalent to

$$\partial_X \eta_i(X, t) \neq 0, \quad \text{for all } X \text{ and } t, \quad i = 1, 2. \quad (12)$$

It is well-known that as long as characteristics do not cross, system (9) has a global smooth solution (w_1, w_2) , provided the initial data is smooth. Differentiate (11) with respect to X ,

$$\partial_x w_i(\eta_i(X, t), t) \partial_X \eta_i(X, t) = \partial_X w_i(X, 0), \quad i = 1, 2,$$

to observe that the condition (12) is equivalent to the non-blow-up in finite time of $\|w_{i,x}\|_{L^\infty}$, $i = 1, 2$.

A priori estimates. We prove below that if at $t = 0$ and for $i = 1, 2$ we have $w_i \in L^\infty$, $w_{i,x} \in L^1$, and $w_{i,xx} \in L^1$, then $\|w_{i,xx}\|_{L^1}$ cannot blow up in finite time. This implies the non-blow-up in finite time of $\|w_{i,x}\|_{L^\infty}$, $i = 1, 2$.

L[∞]-estimate on w_i . From (11) we conclude that, as long as (9) has a smooth solution, it satisfies:

$$\|w_i(\cdot, t)\|_{L^\infty} = \|w_i(\cdot, 0)\|_{L^\infty}, \quad t > 0, \quad i = 1, 2. \quad (13)$$

Using

$$v = \frac{1}{2}(w_1 + w_2) \quad (14a)$$

$$\rho = \exp\left(\frac{w_1 - w_2}{2\sqrt{\kappa}}\right), \quad (14b)$$

we can now obtain uniform bounds in time for $\|v(\cdot, t)\|_{L^\infty}$ and $\|\rho(\cdot, t)\|_{L^\infty}$. Also, some very useful estimates for the variable u (see (3c)) become readily available, as we now show.

For the Green's function G^α given by (6), it is clear that $\|G^\alpha\|_{L^1} = 1$ and $\|G_x^\alpha\|_{L^1} = 1/\alpha$. Now examine the convolution formula (7) for u in terms of v . By Young's inequality, $v \in L^p$ implies $u \in L^p$. In particular, for $v \in L^\infty$, we may use (7) to conclude $u \in L^\infty$, and because $G_x^\alpha \in L^1$, we know that u_x exists and can be computed via $u_x = G_x^\alpha * v$. Using these facts, the following estimates are immediate:

$$\|u\|_{L^\infty} \leq \|G^\alpha\|_{L^1} \|v\|_{L^\infty} = \|v\|_{L^\infty}, \quad (15a)$$

$$\|u_x\|_{L^\infty} \leq \|G_x^\alpha\|_{L^1} \|v\|_{L^\infty} = \frac{1}{\alpha} \|v\|_{L^\infty}, \quad (15b)$$

$$\|u_{xx}\|_{L^\infty} = \frac{1}{\alpha^2} \|u - v\|_{L^\infty} \leq \frac{2}{\alpha^2} \|v\|_{L^\infty}. \quad (15c)$$

L¹-estimate on $w_{i,x}$. Differentiate (9a) with respect to x , multiply by $\text{sgn}(w_{1,x})$ and integrate over the x domain to obtain:

$$\int \partial_t |w_{1,x}| dx + \int (\lambda_2 w_{1,x})_x \text{sgn}(w_{1,x}) dx = 0.$$

The second term in the left-hand side of the equation above is zero. Hence,

$$\|w_{1,x}(\cdot, t)\|_{L^1} = \|w_{1,x}(\cdot, 0)\|_{L^1}, \quad t > 0. \quad (16)$$

Clearly, a similar equation holds for w_2 , so we have

$$\|w_{i,x}(\cdot, t)\|_{L^1} = \|w_{i,x}(\cdot, 0)\|_{L^1}, \quad t > 0, \quad i = 1, 2. \quad (17)$$

Using (14), one can also derive uniform bounds in time for $\|v_x(\cdot, t)\|_{L^1}$ and $\|\rho_x(\cdot, t)\|_{L^1}$.

L¹-estimate on $w_{i,xx}$. Differentiate (9a) twice with respect to x , multiply by $\text{sgn}(w_{1,xx})$ and integrate over the x domain to obtain:

$$\begin{aligned} \frac{d}{dt} \int |w_{1,xx}| dx &= - \int (\lambda_2 w_{1,x})_{xx} \text{sgn}(w_{1,xx}) dx \\ &= - \int (\lambda_2 w_{1,xx})_x \text{sgn}(w_{1,xx}) dx - \int \lambda_{2,x} w_{1,xx} \text{sgn}(w_{1,xx}) dx \\ &\quad - \int \lambda_{2,xx} w_{1,x} \text{sgn}(w_{1,xx}) dx. \end{aligned} \quad (18)$$

The first term in the right-hand side of (18) is zero. We estimate the remaining two terms:

$$\int \lambda_{2,x} w_{1,xx} \text{sgn}(w_{1,xx}) dx \leq \int |\lambda_{2,x}| |w_{1,xx}| dx \leq \|\lambda_{2,x}\|_{L^\infty} \|w_{1,xx}\|_{L^1}, \quad (19)$$

and

$$\int \lambda_{2,xx} w_{1,x} \text{sgn}(w_{1,xx}) dx \leq \int |\lambda_{2,xx}| |w_{1,x}| dx \leq \|\lambda_{2,xx}\|_{L^\infty} \|w_{1,x}\|_{L^1}. \quad (20)$$

Since $c = \sqrt{k}$ is constant, we have $\lambda_{2,x} = u_x$ and $\lambda_{2,xx} = u_{xx}$. By (13) and (14a), we know that $\|v\|_{L^\infty}$ is uniformly bounded in time by a constant that depends only on the L^∞ -norms of

$w_1(\cdot, 0)$ and $w_2(\cdot, 0)$. Putting this together with (15), we conclude that $\|\lambda_{2,x}\|_{L^\infty}$ and $\|\lambda_{2,xx}\|_{L^\infty}$ are bounded by constants that depend only on α , $\|w_1(\cdot, 0)\|_{L^\infty}$ and $\|w_2(\cdot, 0)\|_{L^\infty}$. Using these facts and (16), (19), (20) in (18), we derive:

$$\frac{d}{dt} \int |w_{1,xx}| dx \leq C_1 \int |w_{1,xx}| dx + C_2, \quad (21)$$

where C_1, C_2 depend only on α and the initial data $w_1(\cdot, 0)$ and $w_2(\cdot, 0)$.

Clearly, a similar estimate holds for w_2 as well. One can now use Gronwall's lemma in (21) and in the similar estimate for w_2 to infer the boundedness for finite times of $\|w_{i,xx}\|_{L^1}$, $i = 1, 2$. The Sobolev imbedding $W^{1,1}(\mathbb{R}) \subset L^\infty(\mathbb{R})$ then guarantees the finite-time L^∞ -boundedness of $w_{i,x}$, $i = 1, 2$.

As mentioned earlier, this non-blow-up condition on $\|w_{i,x}\|_{L^\infty}$, $i = 1, 2$, is precisely what is needed to show that characteristics cannot cross in finite time and conclude the global in time existence of a solution of (9), and hence of (3).

Let S be the subset of weakly differentiable functions $f : \mathbb{R} \rightarrow \mathbb{R}$ such that $f \in L^\infty(\mathbb{R})$ and $f' \in W^{1,1}(\mathbb{R})$. For the above a priori estimates to hold, it is sufficient to take initial data such that $w_i(\cdot, 0) \in S$ for $i = 1, 2$. In this case, the a priori estimates derived above guarantee the existence of a unique global solution (w^1, w^2) to (9) such that $(w^1, w^2) \in S \times S$. It follows from remarks made above that both v and ρ have the same regularity as w^j . The following theorem has been proved.

Theorem 1. *Given initial data ρ_0, v_0 such that $w_i(\cdot, 0) \in S$, $i = 1, 2$, there exists a unique global solution $(\rho, v) \in S \times S$ to the initial-value problem (3)-(5).*

Next we show that if $w_i(\cdot, 0)$ itself is a member of L^1 , then w_i remains in L^1 for finite times. From (9a) we may derive

$$\frac{d}{dt} \int |w_1| dx \leq \|u + \sqrt{\kappa}\|_{L^\infty} \int |w_{1,x}| dx \leq C,$$

where the constant C depends only on the initial data $w_1(\cdot, 0)$ and $w_2(\cdot, 0)$. For the last inequality we used the uniform boundedness of $\|v\|_{L^\infty}$, (15a) and (16). A similar result holds for w_2 and thus we have L^1 -control of w_i for finite times:

$$\|w_i(\cdot, t)\|_{L^1} \leq \|w_i(\cdot, 0)\|_{L^1} + Ct, \quad t > 0, \quad i = 1, 2.$$

The L^1 -control of v for finite times follows immediately from (14a). The analogous L^1 estimate for ρ can be derived from the ρ_t equation in (3a), using the uniform boundedness of $\|u\|_{L^\infty}$, $\|\rho\|_{L^\infty}$, $\|v_x\|_{L^1}$ and $\|\rho_x\|_{L^1}$.

Now suppose that $w_i(\cdot, 0) \in W^{2,1}(\mathbb{R})$ for $i = 1, 2$. In this case, the Sobolev imbedding theorem guarantees that $w_i \in L^\infty(\mathbb{R})$, so $w_i \in S$ and the hypotheses of Theorem 1 are satisfied. Based on the arguments presented in the previous paragraph, this is sufficient to conclude that $(w^1, w^2) \in W^{2,1}(\mathbb{R}) \times W^{2,1}(\mathbb{R})$, which in turn implies that $(\rho, v) \in W^{2,1}(\mathbb{R}) \times W^{2,1}(\mathbb{R})$. What we have shown can be summarized in the following extension of Theorem 1.

Theorem 1'. *Given initial data ρ_0, v_0 such that $w_i(\cdot, 0) \in W^{2,1}(\mathbb{R})$, $i = 1, 2$, there exists a unique global solution $(\rho, v) \in W^{2,1}(\mathbb{R}) \times W^{2,1}(\mathbb{R})$ to the initial-value problem (3)-(5).*

Remark. It is interesting to note that (13) and (14b) also imply that ρ is bounded away from zero. The impossibility of vacuum formation is consistent with the Euler equations for a γ -law gas with $\gamma = 1$ (see [Smo83]).

3 The $\alpha \rightarrow 0$ limit

Consider the system (3) subject to initial data (5). Suppose the hypotheses of Theorem 1 are satisfied and denote by (ρ^α, v^α) the unique solution to the Cauchy problem (3)-(5). Now we can formulate the question: what happens to ρ^α , v^α and $u^\alpha(x, t) = \mathcal{H}^{-1}v^\alpha(x, t)$ in the limit as $\alpha \rightarrow 0$?

In what follows, we work with system (4) with initial data $\rho^\alpha(x, 0) = \rho_0(x)$ and $u^\alpha(x, 0) = \mathcal{H}^{-1}v_0(x)$. This is equivalent to working with system (3) with initial data (5). We want to investigate if ρ^α and u^α converge in some sense to a solution of the compressible Euler system.

It is important to remember that as we repeatedly solve (3) with decreasing values of α , the initial data v_0 stays fixed. How does this affect $u^\alpha(x, 0)$? To answer this, simply note that using the Green's function G^α of the operator \mathcal{H} , we may write $u^\alpha(x, 0) = (G^\alpha * v_0)(x)$. We have $\|G^\alpha\|_{L^1} = 1$, while v_0 is bounded and continuous, for all $\alpha > 0$. Then it is a standard property of convolutions (see [Fol99, Thm. 8.14]) that as $\alpha \rightarrow 0$, $u^\alpha(\cdot, 0) \rightarrow v_0$ uniformly on compact subsets of \mathbb{R} .

A compactness argument. Our next step is to use the a priori estimates from the previous section to prove estimates uniform in α for solutions (ρ^α, v^α) to (3). The uniform L^∞ and BV bounds that we are about to show will enable us to pass to the $\alpha \rightarrow 0$ limit by a standard compactness argument; we then study if the resulting limit is a weak solution of the isothermal Euler system.

Proposition 1. *Provided the initial data (ρ_0, v_0) satisfies the hypotheses of Theorem 1, the resulting solution (ρ^α, v^α) satisfies*

$$\|\rho^\alpha(\cdot, \cdot)\|_{L^\infty} \leq M_1, \tag{P1}$$

$$\text{T. V. } \rho^\alpha(\cdot, t) \leq M_2, \tag{P2}$$

$$\|\rho^\alpha(\cdot, t+k) - \rho^\alpha(\cdot, t)\|_{L^1} \leq M_3 k, \quad \text{for any } k > 0, \tag{P3}$$

and

$$\|v^\alpha(\cdot, \cdot)\|_{L^\infty} \leq M'_1, \tag{P1'}$$

$$\text{T. V. } v^\alpha(\cdot, t) \leq M'_2, \tag{P2'}$$

$$\|v^\alpha(\cdot, t+k) - v^\alpha(\cdot, t)\|_{L^1} \leq M'_3 k, \quad \text{for any } k > 0, \tag{P3'}$$

for any $t \in [0, T]$. Here, M_1, M'_1 are independent of α , M_2, M'_2 are independent of t and α and M_3, M'_3 are independent of t, k and α .

Proof. From Section 2, as consequences of (13), (14) and (15a), we have uniform in α bounds on $\|v^\alpha(\cdot, t)\|_{L^\infty}$, $\|u^\alpha(\cdot, t)\|_{L^\infty}$ and $\|\rho^\alpha(\cdot, t)\|_{L^\infty}$. We can also derive from (13), (17) and (14) uniform in α bounds on $\|v_x^\alpha(\cdot, t)\|_{L^1}$ and $\|\rho_x^\alpha(\cdot, t)\|_{L^1}$. In turn, the uniform bounds on $\|v_x^\alpha(\cdot, t)\|_{L^1}$ and $\|\rho_x^\alpha(\cdot, t)\|_{L^1}$ yield uniform bounds on the total variations T.V. v^α and T.V. ρ^α .

Also, by integrating (3a) with respect to time from t to $t+k$ ($k > 0$) we obtain

$$\begin{aligned} \int_{\mathbb{R}} |\rho^\alpha(x, t+k) - \rho^\alpha(x, t)| dx &\leq \int_{\mathbb{R}} \int_t^{t+k} (|u^\alpha \rho_x^\alpha| + |\rho^\alpha v_x^\alpha|) dx ds \\ &\leq k (\|u^\alpha\|_{L^\infty} \|\rho_x^\alpha\|_{L^1} + \|\rho^\alpha\|_{L^\infty} \|v_x^\alpha\|_{L^1}) \\ &\leq M_3 k, \end{aligned} \tag{22}$$

and

$$\begin{aligned} \int_{\mathbb{R}} |v^\alpha(x, t+k) - v^\alpha(x, t)| dx &\leq \int_{\mathbb{R}} \int_t^{t+k} (|u^\alpha v_x^\alpha| + \kappa |1/\rho^\alpha \rho_x^\alpha|) dx ds \\ &\leq k (\|u^\alpha\|_{L^\infty} \|v_x^\alpha\|_{L^1} + \kappa \|1/\rho^\alpha\|_{L^\infty} \|\rho_x^\alpha\|_{L^1}) \\ &\leq M'_3 k, \end{aligned} \tag{23}$$

where M_3 and M'_3 do not depend on α , but only on the initial data ρ_0, v_0 . Here we used the previous observations regarding the uniform L^∞ -bounds of ρ^α and u^α and the L^1 -bounds of ρ_x^α and v_x^α . Note that the uniform lower bound of $\|\rho^\alpha\|_{L^\infty}$ also follows from (13) and (14). \square

Using the two sets of properties (P1)-(P3) and (P1')-(P3') we can establish

Theorem 2. *Suppose we solve the Cauchy problem (3)-(5) with an initial data satisfying the hypotheses of Theorem 1. Then, as $\alpha \rightarrow 0$, passing if necessary to a subsequence, there exist two functions $\rho(x, t)$ and $u(x, t)$ such that*

$$\rho^\alpha \rightarrow \rho \text{ in } C([0, \infty); L^1_{\text{loc}}(\mathbb{R})) \tag{24}$$

and

$$v^\alpha \rightarrow u \text{ in } C([0, \infty); L^1_{\text{loc}}(\mathbb{R})). \tag{25}$$

Proof. The theorem concerns compactness, i.e. strong convergence of ρ^α and v^α in the zero- α limit. The two sets of uniform estimates proved in Proposition 1 are precisely the conditions of the L^1 compactness theory for conservation laws — see [HR02, Thm. A.8] or [Smo83, Thm. 19.9] for modern accounts of this. This enables us to construct a subsequence $\alpha_j \rightarrow 0$ such that $\{\rho^{\alpha_j}(t)\}, \{v^{\alpha_j}(t)\}$ converge strongly to functions $\rho(x, t)$ and $u(x, t)$, respectively, where $\rho(\cdot, t), u(\cdot, t) \in L^1_{\text{loc}}(\mathbb{R})$ for each $t \geq 0$. The convergence is in $C([0, \infty); L^1_{\text{loc}}(\mathbb{R}))$. \square

We show in the following proposition that $u^\alpha(x, t) = \mathcal{H}^{-1}v^\alpha(x, t)$ also converges to u in $C([0, \infty); L^1_{\text{loc}}(\mathbb{R}))$.

Proposition 2. *Let u be the limit on a subsequence of v^α , as derived in Theorem 2. Then,*

$$u^\alpha \rightarrow u \text{ in } C([0, \infty), L^1_{\text{loc}}(\mathbb{R})), \tag{26}$$

on the same subsequence.

Proof. Considering (25), it is enough to show

$$\sup_{[0, T]} \int_K |u^\alpha - v^\alpha| dx \rightarrow 0, \quad \text{as } \alpha \rightarrow 0, \tag{27}$$

for any finite time T and compact K . We have

$$\int_K |u^\alpha - v^\alpha| dx = \int_K \left| \frac{1}{2\alpha} \int_{\mathbb{R}} e^{-|x-y|/\alpha} v^\alpha(y, t) dy - v^\alpha(x, t) \right| dx.$$

Here, we used $u^\alpha = G^\alpha * v^\alpha$. Integrating by parts, we get

$$\frac{1}{2\alpha} \int_{\mathbb{R}} e^{-|x-y|/\alpha} v^\alpha(y, t) dy = v^\alpha(x, t) + \frac{1}{2} \int_{\mathbb{R}} \operatorname{sgn}(y-x) e^{-|y-x|/\alpha} v_y^\alpha(y, t) dy.$$

Continuing, we find

$$\begin{aligned} \int_K |u^\alpha - v^\alpha| dx &\leq \frac{1}{2} \int_K \int_{\mathbb{R}} e^{-|y-x|/\alpha} |v_y^\alpha(y, t)| dy dx \\ &= \frac{1}{2} \int_K |v_y^\alpha(y, t)| dy \int_{\mathbb{R}} e^{-|y-x|/\alpha} dx \\ &= \alpha \int_K |v_y^\alpha(y, t)| dy. \end{aligned}$$

The term

$$\int_K |v_y^\alpha(y, t)| dy$$

is uniformly bounded with respect to $t \in [0, T]$ and α — see (P2'). Hence, (27) follows and the argument is complete. \square

Strong convergence to a weak solution of the isothermal Euler equations? In this paragraph we consider the solution (ρ^α, u^α) of the Leray system (4) and study if its limit (ρ, u) represents a weak solution of the compressible Euler system for an isothermal gas given by (1).

Considering that the system (4) is not in conservation law form, the answer to this question is not immediate. In fact we can prove only a partial result, i.e. (ρ, u) is a weak solution of the momentum equation (1b). It seems that we do not have sufficient properties on the sequences ρ^α and u^α to conclude that (ρ, u) is a weak solution of the continuity equation (1a) as well and we will give a formal argument on why we believe that in fact this is not actually true.

The next proposition contains the positive half of the result.

Proposition 3. *The limit (ρ, u) established in Theorem 2 is a global weak solution of (1b), i.e. the momentum equation of the compressible Euler system for an isothermal gas.*

Proof. We use equation (4b), which we repeat here using superscripts α :

$$u_t^\alpha + u^\alpha u_x^\alpha + \kappa \frac{\rho_x^\alpha}{\rho^\alpha} - \alpha^2 u_{txx}^\alpha - \alpha^2 u^\alpha u_{xxx}^\alpha = 0. \quad (28)$$

We wish to prove that the α^2 terms

$$\alpha^2 u_{txx}^\alpha + \alpha^2 u^\alpha u_{xxx}^\alpha,$$

converge weakly to 0 as $\alpha \rightarrow 0$. Suppose we have shown this; then, we may multiply (28) by a test function φ that is compactly supported in $\mathbb{R} \times [0, \infty)$ and integrate in space and time. Now

taking $\alpha \rightarrow 0$, we will find that the order α^2 terms vanish, and we are left with a function u that satisfies

$$\int_0^\infty \int_{\mathbb{R}} u \varphi_t + \frac{1}{2} u^2 \varphi_x + \kappa \log \rho \varphi_x \, dx \, dt = 0,$$

for all compactly supported φ . This is precisely the statement that (ρ, u) is a global weak solution of the momentum equation (1b), and would prove the proposition.

For the first α^2 term from (28), we have, for any compactly supported φ ,

$$\alpha^2 \int_0^T \int_{\mathbb{R}} u_{txx}^\alpha \varphi \, dx \, dt = -\alpha^2 \int_0^T \int_{\mathbb{R}} u^\alpha \varphi_{txx} \, dx \, dt.$$

Using the convergence of the sequence u^α , it is clear that this term converges to 0 as $\alpha \rightarrow 0$. For the second α^2 term from (28), we may derive using integration by parts

$$\alpha^2 \int_0^T \int_{\mathbb{R}} u^\alpha u_{xxx}^\alpha \varphi \, dx \, dt = \frac{1}{4} \alpha^2 \int_0^T \int_{\mathbb{R}} (u^\alpha)^2 \varphi_{xxx} \, dx \, dt - \frac{3}{2} \alpha^2 \int_0^T \int_{\mathbb{R}} u^\alpha u_{xx}^\alpha \varphi_x \, dx \, dt. \quad (29)$$

By using the boundedness and the convergence of u^α , we conclude that the first term on the right-hand side of (29) vanishes in the $\alpha \rightarrow 0$ limit. Regarding the second term, by considering the boundedness of u^α , it is enough to show that

$$\alpha^2 \int_0^T \int_K |u_{xx}^\alpha| \, dx \rightarrow 0,$$

for any compact K . But this follows from (25) and (26), where one uses $\alpha^2 u_{xx}^\alpha = u^\alpha - v^\alpha$. \square

Consider now (4a), which we repeat with superscripts α :

$$\rho_t^\alpha + (\rho^\alpha u^\alpha)_x - \alpha^2 \rho^\alpha u_{xxx}^\alpha = 0. \quad (30)$$

Can we pass to the limit $\alpha \rightarrow 0$ in (30) and conclude that (ρ, u) established in Theorem 2 is a global weak solution of (1a)? Yes, provided the α^2 term, $\alpha^2 \rho^\alpha u_{xxx}^\alpha$ converges weakly to 0 as $\alpha \rightarrow 0$.

Integrating by parts we have

$$\alpha^2 \int_0^T \int_K \rho^\alpha u_{xxx}^\alpha \varphi \, dx \, dt = -\alpha^2 \int_0^T \int_K \rho_x^\alpha u_{xx}^\alpha \varphi \, dx \, dt - \alpha^2 \int_0^T \int_K \rho^\alpha u_{xx}^\alpha \varphi_x \, dx \, dt, \quad (31)$$

for any test function φ with support K . The second term in the right-hand-side goes to 0 as $\alpha \rightarrow 0$, due to an argument similar to that used to conclude that the second term on the right-hand side of (29) vanishes in the $\alpha \rightarrow 0$ limit. We only need to use the uniform boundedness of ρ^α instead.

It seems however that we do not have enough properties on ρ^α and u^α to conclude that the first term on the right-hand-side of (31) vanishes in the $\alpha \rightarrow 0$ limit. We list the relevant properties of ρ^α and u^α here:

$$\|\rho^\alpha\|_{L^\infty} \leq M_1, \quad \|\rho_x^\alpha\|_{L^1} \leq M_2, \quad \rho^\alpha \rightarrow \rho \text{ in } C([0, \infty); L_{\text{loc}}^1(\mathbb{R})),$$

and

$$\|u^\alpha\|_{L^\infty} \leq M'_1, \quad \|u_x^\alpha\|_{L^1} \leq M'_2, \quad \|\alpha^2 u_{xx}^\alpha\|_{L^1} \rightarrow 0 \text{ in } C([0, \infty); L^1_{\text{loc}}(\mathbb{R})).$$

We expect that ρ_x^α and u_x^α converge to the Dirac δ distribution at the shock, that is $\rho^\alpha \sim \Psi_1\left(\frac{x}{\alpha}\right)$, with $\rho_x^\alpha \sim \frac{1}{\alpha}\Psi_1\left(\frac{x}{\alpha}\right)$, and $u^\alpha \sim \Psi_2\left(\frac{x}{\alpha}\right)$, with $u_x^\alpha \sim \frac{1}{\alpha}\Psi_2\left(\frac{x}{\alpha}\right)$. Here, Ψ_1 and Ψ_2 are smooth functions with compact support such that $\int \Psi_1 dx = 1$ and $\int \Psi_2 dx = 1$. Note that the above properties on the L^∞ and L^1 -norms of ρ^α , u^α and their derivatives are satisfied when ρ^α and u^α are in this form. We also have $\alpha^2 u_{xx}^\alpha \sim \Psi_2'\left(\frac{x}{\alpha}\right)$ and hence

$$\|\alpha^2 u_{xx}^\alpha\|_{L^1} \sim \int \left| \Psi_2'\left(\frac{x}{\alpha}\right) \right| dx = \alpha \int |\Psi_2'(y)| dy.$$

Provided $\|\Psi_2'\|_{L^1}$ is finite, we have $\|\alpha^2 u_{xx}^\alpha\|_{L^1} \rightarrow 0$, as needed. There is no reason however to expect the first term on the right-hand-side of (31) to vanish in the $\alpha \rightarrow 0$ limit, for ρ^α , u^α in this form. Indeed, ignoring the time dependence,

$$\begin{aligned} \alpha^2 \int \rho_x^\alpha u_{xx}^\alpha \varphi dx &\sim \frac{1}{\alpha} \int \Psi_1\left(\frac{x}{\alpha}\right) \Psi_2'\left(\frac{x}{\alpha}\right) \varphi dx \\ &= \int \Psi_1(y) \Psi_2'(y) \varphi(\alpha y) dy. \end{aligned}$$

If we choose φ to be equal to 1 in the interior of a compact set and 0 outside, then the integral above does not vanish as $\alpha \rightarrow 0$. Though this is only a formal argument, we nevertheless conjecture that the Leray regularization does not capture entropy solutions of the compressible Euler equations for an isothermal gas. This conjecture is supported by the numerical results of the next section.

4 Numerical results

This section contains numerical results confirming that the Leray regularization does not capture entropy solutions of the isothermal Euler equations. The numerical experiments are performed using a discretization based on the Riemann invariant system (10)-(11). By discretizing the characteristic form of the equations, we produce a numerical method that preserves the monotonicity of the characteristics, an important feature for long-time integration.

Numerical method. We wish to integrate the equations (10), which can be written as

$$\dot{\eta}_1(X, t) = u(\eta_1(X, t), t) + c \tag{32a}$$

$$\dot{\eta}_2(X, t) = u(\eta_2(X, t), t) - c. \tag{32b}$$

Our goal now is to rewrite $u \circ \eta_j$ in such a way that it can be evaluated using only $\eta_1(X, t)$, $\eta_2(X, t)$, and the initial data for the problem. It is not obvious that this is possible, so we outline the procedure. In the relationship between u and v , given by (7), we use (14a) to obtain

$$u(x, t) = \frac{1}{4\alpha} \int_{\mathbb{R}} e^{-|x-y|/\alpha} [w_1(y, t) + w_2(y, t)] dy.$$

We split the integral into two pieces

$$u(x, t) = \frac{1}{4\alpha} \int_{\mathbb{R}} e^{-|x-y|/\alpha} w_1(y, t) dy + \frac{1}{4\alpha} \int_{\mathbb{R}} e^{-|x-y|/\alpha} w_2(y, t) dy.$$

In the first integral, we substitute $y = \eta_1(Y, t)$. In the second integral, we substitute $y = \eta_2(Y, t)$. We use (11) and set $x = \eta_j(X, t)$. This gives expressions for $u(\eta_j(X, t), t)$, which we then substitute into the right-hand side of (32). We thereby obtain

$$\begin{aligned} \dot{\eta}_j(X, t) = & (-1)^{j+1} c + \frac{1}{4\alpha} \int_{\mathbb{R}} e^{-|\eta_j(X, t) - \eta_1(Y, t)|/\alpha} w_1(Y, 0) \partial_Y \eta_1(Y, t) dY \\ & + \frac{1}{4\alpha} \int_{\mathbb{R}} e^{-|\eta_j(X, t) - \eta_2(Y, t)|/\alpha} w_2(Y, 0) \partial_Y \eta_2(Y, t) dY. \end{aligned} \quad (33)$$

Together with the initial conditions $\eta_j(X, 0) = X$, this is a closed system of equations for $\eta_1(X, t)$ and $\eta_2(X, t)$. If we now discretize this system in time and space, we have a purely Lagrangian scheme for solving the Leray system.

Assume first that $w_j(X, 0)$ vanishes as $|X| \rightarrow \infty$. Then it is possible to choose an interval $[a, b]$ so that $w_j(X, 0)$ is negligible for $X \notin [a, b]$. This justifies truncating the domains of integration from \mathbb{R} to $[a, b]$, resulting in

$$\begin{aligned} \dot{\eta}_j(X, t) = & (-1)^{j+1} c + \frac{1}{4\alpha} \int_a^b e^{-|\eta_j(X, t) - \eta_1(Y, t)|/\alpha} w_1(Y, 0) \partial_Y \eta_1(Y, t) dY \\ & + \frac{1}{4\alpha} \int_a^b e^{-|\eta_j(X, t) - \eta_2(Y, t)|/\alpha} w_2(Y, 0) \partial_Y \eta_2(Y, t) dY. \end{aligned} \quad (34)$$

Again under the assumption that $w_j(X, 0)$ vanishes as $|X| \rightarrow \infty$, we see that for $|X|$ sufficiently large we have, asymptotically in X , $\dot{\eta}_j(X, t) \sim (-1)^{j+1} c$. Integrating both sides with respect to t and using $\eta_j(X, 0) = X$ we find that $\eta_j(X, t) \sim (-1)^{j+1} ct + X$. Therefore,

$$\partial_X \eta_j(X, t) \sim 1 \quad (35)$$

asymptotically in X for $|X|$ sufficiently large. We will use this fact shortly.

Discretization in space. The next step is to approximate the integrals and derivatives in (34). Fix N . For $0 \leq i \leq N$, define $X_i = a + i\Delta x$ where $\Delta x = (b - a)/N$. Let $\eta_{j,i}(t)$ denote the numerical approximation to $\eta_j(X_i, t)$ on the interval $[a, b]$, and let $\boldsymbol{\eta}_j(t) = (\eta_{j,0}(t), \dots, \eta_{j,N}(t))$. In the present study, we use a 7-point, 5th order finite difference formula to approximate first derivatives in space. That is, we approximate ∂_Y by the $(N+1) \times (N+1)$ antisymmetric matrix $D_1 = (M - M^T)/\Delta x$ where M has the entries $(3/4, -3/20, 1/60)$ on the first, second, and third superdiagonals, respectively. Since the first three and last three rows of D_1 cannot possibly contain the full 7-point stencil, when we compute $D_1 \boldsymbol{\eta}_j$, the first three and last three entries will be incorrect. To remedy this, we use the asymptotic expression (35) to replace these incorrect entries by 1. Let $\tilde{D}_1 \boldsymbol{\eta}_j$ denote the derivative vector obtained after fixing $D_1 \boldsymbol{\eta}_j$ in this way.

We now have a choice of quadrature rules to approximate the integrals in (34). In the present study, we use the trapezoidal rule. Applying the above spatial discretizations to (34), we obtain

$$\dot{\eta}_{j,i} = (-1)^{j+1} c + \frac{\Delta x}{8\alpha} \sum_{k=0}^N \sigma_k \left[e^{-|\eta_{j,i} - \eta_{1,k}|/\alpha} w_{1,k} \left(\tilde{D}_1 \boldsymbol{\eta}_1 \right)_k + e^{-|\eta_{j,i} - \eta_{2,k}|/\alpha} w_{2,k} \left(\tilde{D}_1 \boldsymbol{\eta}_2 \right)_k \right], \quad (36)$$

where $w_{j,k} = w_j(X_k, 0)$ and

$$\sigma_k = \begin{cases} 1 & k = 0 \\ 2 & 1 \leq k \leq N - 1 \\ 1 & k = N. \end{cases}$$

Monotonicity. Note that (36) is a system of $N + 1$ coupled nonlinear ordinary differential equations which we can abbreviate as $\dot{\boldsymbol{\eta}}_j = f_j(\boldsymbol{\eta}_1, \boldsymbol{\eta}_2)$. The system is well-posed: for $j = 1$ and $j = 2$, we have that f_j is differentiable and that the partial derivatives $\partial f_j / \partial \eta_{j,i}$ are all bounded. Hence f_j is Lipschitz and the standard existence and uniqueness theorem for ODEs can be applied.

We know that the true characteristic curves satisfy $\eta_i(X, 0) = X$, which implies $\partial_X \eta_i(X, 0) = 1$. From the well-posedness results in Section 2, we get $\partial_X \eta_i(X, t) > 0$ for all $t \geq 0$. In other words, for each fixed $t \geq 0$, $\eta_i(X, t)$ is a monotonic function of X . It is of interest to show that (36) respects the monotonicity of η_j in a discrete sense:

Proposition 4. *Suppose $\eta_{j,i+1}(0) > \eta_{j,i}(0)$ for each $i = 0, 1, \dots, N - 1$. Then under the dynamics of (36), we have $\eta_{j,i+1}(t) > \eta_{j,i}(t)$ for each $i = 0, 1, \dots, N - 1$ and for all $t > 0$.*

Proof. Define $s_{j,i}(t) = \eta_{j,i+1}(t) - \eta_{j,i}(t)$ for $0 \leq i \leq N - 1$. Using (36),

$$\begin{aligned} \dot{s}_{j,i} = \frac{\Delta x}{8\alpha} \sum_{k=0}^N \sigma_k & \left\{ \left[e^{-|\eta_{j,i+1} - \eta_{1,k}|/\alpha} - e^{-|\eta_{j,i} - \eta_{1,k}|/\alpha} \right] w_{1,k} \left(\tilde{D}_1 \boldsymbol{\eta}_1 \right)_k \right. \\ & \left. + \left[e^{-|\eta_{j,i+1} - \eta_{2,k}|/\alpha} - e^{-|\eta_{j,i} - \eta_{2,k}|/\alpha} \right] w_{2,k} \left(\tilde{D}_1 \boldsymbol{\eta}_2 \right)_k \right\}. \end{aligned}$$

It is a simple exercise to rewrite the right-hand side as a function of the $s_{j,i}$ only, and thereby show that the standard existence and uniqueness theorem applies to the $\dot{s}_{j,i}$ dynamical system.

Now fix i . Suppose $s_{j,i} = 0$, so that $\eta_{j,i+1} = \eta_{j,i}$. Then it is clear that in the above expression, each of the terms in square brackets vanishes. In this case, $\dot{s}_{j,i} = 0$. Therefore, given the initial time $t_0 \in \mathbb{R}$ and the initial condition $s_{j,i}(t_0) = 0$, we see that the unique solution of the $\dot{s}_{j,i}$ equation is $s_{j,i}(t) \equiv 0$ for all t . By uniqueness of solutions, the initial condition $s_{j,i}(0) > 0$ necessarily implies $s_{j,i}(t) > 0$ for all t , finishing the proof. \square

Remarks:

1. To restate the argument from the above proof in a geometric way, we can say that the phase space for the $\dot{\mathbf{s}}_1, \dot{\mathbf{s}}_2$ dynamical system is sliced by $2N$ invariant hyperplanes of the form $s_{j,i} = 0$. It is impossible for trajectories that start on one side of one of these hyperplanes to cross over to the other side.
2. Note that in practice, we will always use (36) with the initial condition $\eta_{j,i}(0) = X_i$, so that $\eta_{j,i+1}(0) - \eta_{j,i}(0) = \Delta x > 0$ and the condition of the above proposition is satisfied.
3. We can prove the monotonicity result in precisely the same way if instead of the trapezoidal rule we use the lower-order rectangle rule to evaluate the integrals in (34). However, the proof fails if we use the higher-order Simpson rule. We have not explored generalizations involving quadrature on non-equispaced grids.

Discretization in time. In the present study, we will use a standard fourth-order Runge-Kutta method to solve the ODE system (36). In future work, we hope to analyze the errors incurred by the specific choice of spatial and temporal discretizations made here.

Convergence of the method. In the absence of a proof of convergence for the numerical method, we carry out a numerical test. Each choice of initial data we present below will depend on a real parameter δ . For each choice of initial data, we freeze the values of α and δ and then repeatedly run simulations with increasing values of N (the number of particles) and decreasing values of the timestep Δt . We take as a reference solution the numerical solution computed with the largest space and time resolution: $N = 4001$, $\Delta t = 0.0025$. We compute the relative L^2 errors at the final time $T = 4$ between the reference solution and the numerical solutions obtained for (a) $N = 251$, $\Delta t = 0.04$, (b) $N = 501$, $\Delta t = 0.02$, (c) $N = 1001$, $\Delta t = 0.01$ and (d) $N = 2001$, $\Delta t = 0.005$.

Let e_j denote the computed relative error for η_j , $j = 1, 2$. Then we observe that $\log e_j$ plotted versus $\log(\Delta t^2/N)$ yields a line with slope close to one. Hence, the numerical test of convergence yields a relative error decay of $e_j = C_j(\Delta t)^2 N^{-1}$ for constants C_j , $j = 1, 2$, and gives evidence that the numerical method is converging.

Comparison with finite difference scheme. We also have a finite difference code that solves the Leray system in the ρ and v variables (3) directly. The results of the two numerical methods are in complete agreement for as long as the finite difference code is well-resolved, which can be for fairly long times if fine spatial and temporal resolutions are used. However, as we have found, the finite difference scheme for (3) is not suitable for the long-time integration of problems involving shocks. There are two reasons. First, the scheme does not guarantee the monotonicity of characteristic curves, and second, in the numerical solution of (3), quantities such as $v(x, t)$ tend to steepen exponentially in time, requiring very high resolution and small final times. The characteristic/particle method that we employ circumvents these obstacles.

Numerical results. We consider two types of initial data for the Leray system: Gaussian and front-like initial conditions. We perform these numerical experiments to determine whether these initial profiles evolve into the entropic solutions of the Euler equations. This is a typical test to check if a regularization of the Euler equations is faithful. For the front-like initial data the exact solution of the Euler equations can be computed exactly, while for the Gaussian initial data we use as the entropic solution of the Euler system the numerical solution produced by a numerical conservation law scheme. For this purpose we use the CLAWPACK software package². In all numerical simulations, the parameter κ is taken to be 0.4.

A. Gaussian initial data. We first consider the initial data

$$\mathbf{r}_0 = 1 + 15 \exp\left(-((\mathbf{X} + 0.1)/\delta)^2\right), \quad (37a)$$

$$\mathbf{v}_0 = 0. \quad (37b)$$

Here δ measures the width of the Gaussian. This initial data corresponds to a detonation wave. The initial density consists of a large amplitude disturbance localized around one point while the initial velocity is simply zero.

²CLAWPACK is freely available on a website hosted by the Department of Applied Mathematics at the University of Washington. See <http://www.amath.washington.edu/~claw/>.

Convergence to the Euler solution? Here we address the main question of this study: do the solutions of the Leray system (3) approach the entropic Euler solution as the smoothing parameter α decreases to 0? Here α is the width of the Helmholtz filter (7); we expect that the role of α in the Leray regularization (3) is analogous to the role of viscosity ν in a viscous regularization of the compressible Euler equations.

For successively smaller values of α , we compare the numerical solutions of the Leray system (3) to a reference solution of the Euler system. By reference solution, we mean a high-resolution numerical solution of the isothermal Euler system (1) that we compute using the CLAWPACK package. For the reference solution, we use $N = 10000$ grid points and the initial data (37). Table 1 displays the relative L^2 -errors between the entropic Euler solution as computed by CLAWPACK and the numerical solutions of the Leray system with $\alpha = 0.4, 0.2, 0.1$, and 0.05 . The final time is $T = 4$, δ is fixed at 0.1 and the resolution used for all the runs is $N = 4001$ and $\Delta t = 0.0025$. The plots presented in Figure 1 clearly show that the Leray system fails to capture the shock speed of the entropic Euler solution.

Table 1: Gaussian initial data: convergence to the Euler solution? The table displays the relative L^2 -errors between the entropic Euler solution as computed by CLAWPACK and the numerical solutions of the Leray system for $\alpha = 0.4, 0.2, 0.1, 0.05$ at $T = 4$. For all the runs, $N = 4001$, $\Delta t = 0.0025$, and the initial data is given by (37). Note that the errors approach an order $O(1)$ limit as α approaches 0.

	ρ : relative L^2 -error	v : relative L^2 -error
$\alpha = 0.4$	0.3736	7.9194×10^{-1}
$\alpha = 0.2$	0.3174	6.8900×10^{-1}
$\alpha = 0.1$	0.3017	6.4291×10^{-1}
$\alpha = 0.05$	0.2980	6.2727×10^{-1}

B. Front-like initial data. We consider smoothed Riemann data to initialize our numerical method, that is the initial condition w_1^0, w_2^0 represent smoothed fronts connecting a left state (w_{1L}, w_{2L}) to a right state (w_{1R}, w_{2R}) . The corresponding initial profiles of ρ and v —computed using (14)—also represent smoothed fronts connecting a left state (ρ_L, u_L) to a right state (ρ_R, u_R) . In the numerical experiment presented below, the values ρ_L, u_L, ρ_R and u_R are chosen so that the exact solution of the Euler equations corresponding to the Riemann initial data with these left and right states represent a combination of a 1-shock and a 2-rarefaction waves. Other choices of left and right states lead to similar conclusions.

It is well-known that standard regularizations such as the viscosity method, initialized with smoothed Riemann data profiles, recover the entropic solution of the Euler equations when the viscosity and the parameter controlling the smoothing of the initial data decrease to 0. However, a similar study for the Leray regularization renders a negative result.

For the numerical simulations in this section, we use the smoothed Riemann initial data

$$\mathbf{w}_1^0 = \frac{w_{1R} - w_{1L}}{2} \tanh\left(\frac{\mathbf{X}}{\delta}\right) + \frac{w_{1R} + w_{1L}}{2}, \quad (38a)$$

$$\mathbf{w}_2^0 = \frac{w_{2R} - w_{2L}}{2} \tanh\left(\frac{\mathbf{X}}{\delta}\right) + \frac{w_{2R} + w_{2L}}{2}. \quad (38b)$$

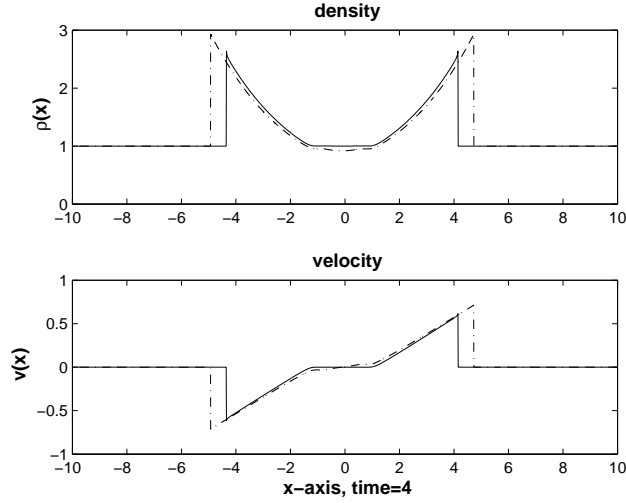


Figure 1: Gaussian initial data. The solid line represents the numerical solution at $T = 4$ of the Leray system with $\alpha = 0.05$, computed using a very fine spacetime grid with $N = 4001$ and $\Delta t = 0.0025$. The dash-dot line represents the entropic solution of the Euler equations computed using CLAWPACK. Note the $O(1)$ error between the two solutions.

Here, δ measures the smoothing in the initial data.

Note that for the front-like initial data, an assumption made earlier in the derivation of the particle method no longer holds. Specifically, since $w_j(X, 0)$ does not approach 0 as $|X| \rightarrow \infty$, we cannot truncate the integrals from (33). In future work, we will explain how to deal with this issue in a systematic way. For now, we employ a solution that is convenient from the point of view of numerical implementation. Namely, we start with (33) and again truncate the domains of integration from \mathbb{R} to a finite interval $[a, b]$. However, when we evaluate these integrals, we include a sufficient number of “ghost” particles that lie to the left of a and to the right of b . In this extension scheme, we assume that the ghost particles move at fixed speeds determined by the boundary values of $w_j(X, 0)$.

With this in mind, assume that $\lim_{X \rightarrow -\infty} w_j(X, 0) = w_{jL}$ and $\lim_{X \rightarrow +\infty} w_j(X, 0) = w_{jR}$. By (14) and (7), this implies that $\rho(X, 0)$, $v(X, 0)$ and $u(X, 0)$ all have right/left limits as $X \rightarrow \pm\infty$, which we will denote using subscript R and L , respectively. Now assume³ that $\lim_{X \rightarrow \pm\infty} \eta(X, t) = \pm\infty$. Then if we take $X \rightarrow \pm\infty$ in (32), we obtain

$$\lim_{X \rightarrow -\infty} \dot{\eta}_j(X, t) = u_L + (-1)^{j+1}c, \quad \lim_{X \rightarrow +\infty} \dot{\eta}_j(X, t) = u_R + (-1)^{j+1}c. \quad (39)$$

Let M be a positive integer denoting the number of ghost particles we wish to add on each side of $[a, b]$. Then we rewrite (36) in the following way:

$$\dot{\eta}_{j,i} = (-1)^{j+1}c + \frac{\Delta x}{8\alpha} \sum_{k=-M}^{N+M} \sigma_k \left[e^{-|\eta_{j,i} - \eta_{1,k}|/\alpha} w_{1,k} \left(\tilde{D}_1 \boldsymbol{\eta}_1 \right)_k + e^{-|\eta_{j,i} - \eta_{2,k}|/\alpha} w_{2,k} \left(\tilde{D}_1 \boldsymbol{\eta}_2 \right)_k \right], \quad (40)$$

³This assumption is true at $t = 0$ and holds for $t > 0$ if we make certain assumptions on the initial data.

where for $-M \leq k \leq -1$, we prescribe the following positions for the M ghost particles to the left of a :

$$\eta_{j,k}(t) = X_k + (u_L + (-1)^{j+1}c) t.$$

Also, for $N+1 \leq k \leq N+M$, we prescribe the following positions for the M ghost particles to the right of b :

$$\eta_{j,k}(t) = X_k + (u_R + (-1)^{j+1}c) t.$$

We take $(\tilde{D}_1 \boldsymbol{\eta}_j)_k = 1$ for $k < 0$ and $k > N$. The above definitions are exact at $t = 0$ and consistent with (39) for $t > 0$. We also extend $w_{j,k}$ and σ_k as follows:

$$w_{j,k} = \begin{cases} w_{jL} & -M \leq k \leq -1 \\ w_j(X_k, 0) & 0 \leq k \leq N \\ w_{jR} & N+1 \leq k \leq N+M \end{cases}$$

$$\sigma_k = \begin{cases} 1 & k = -M \\ 2 & -M+1 \leq k \leq N+M-1 \\ 1 & k = N+M. \end{cases}$$

Note that the monotonicity result proved earlier still applies to (40). We omit further details.

Exact solution of the Euler system. The initial data (38) is intended to be a smoothed version of initial data for which we have an exact solution of the Euler system (1). Here we outline the construction of this exact solution.

Take $\rho_L = 0.1$, $u_L = 0.2$. Now consider the right state (ρ_R, u_R) and an intermediate state (ρ_{int}, u_{int}) such that (ρ_{int}, u_{int}) can be connected to (ρ_L, u_L) on the right by a 1-shock and (ρ_R, u_R) can be connected to (ρ_{int}, u_{int}) on the right by a 2-rarefaction. We take $\rho_{int} = 0.4$, $\rho_R = 0.5$ and compute u_{int} , u_R using standard shock-rarefaction curves⁴:

$$u_{int} = u_L - \sqrt{\frac{\kappa}{\rho_{int}\rho_L}}(\rho_{int} - \rho_L),$$

$$u_R = u_{int} + \sqrt{\kappa} \log \frac{\rho_R}{\rho_{int}}.$$

⁴The calculation of shock and rarefaction curves for the Euler equations for an isothermal gas is standard and we omit to present it here in detail (see the classical monographs [Smo83] or [CF76] for instance). A left state (ρ_L, u_L) can be connected to a right state (ρ, u) by a 1- or a 2-shock, provided the right state is on the following 1- and 2-shock curves, respectively

$$S_1: \quad u - u_L = -\sqrt{\frac{\kappa}{\rho\rho_L}}(\rho - \rho_L), \quad \rho > \rho_L,$$

$$S_2: \quad u - u_L = \sqrt{\frac{\kappa}{\rho\rho_L}}(\rho - \rho_L), \quad \rho < \rho_L.$$

Also, the 1- and 2- rarefaction curves can be computed as

$$R_1: \quad u - u_L = -\sqrt{\kappa} \log \frac{\rho}{\rho_L}, \quad \rho < \rho_L,$$

$$R_2: \quad u - u_L = \sqrt{\kappa} \log \frac{\rho}{\rho_L}, \quad \rho > \rho_L.$$

Here we used the equations for S_1 and R_2 from the footnote.

Therefore, the exact solution of the Euler system is a 1-shock followed by a 2-rarefaction:

$$u_{Euler}(x, t) = \begin{cases} u_L & x < st \\ u_{int} & st < x < \lambda_2(\rho_{int}, u_{int})t \\ \frac{x}{t} - c & \lambda_2(\rho_{int}, u_{int})t < x < \lambda_2(\rho_R, u_R)t \\ u_R & x > \lambda_2(\rho_R, u_R)t, \end{cases} \quad (41)$$

where the 1-shock speed is

$$s = \frac{\rho_{int}u_{int} - r_L u_L}{\rho_{int} - \rho_L}.$$

The expression for ρ follows from the expression for u . The density has a shock transition from ρ_L to ρ_{int} across $x = st$, followed by a rarefaction fan where we need to use R_2 (see the footnote) to get $\rho(x, t)$ from $u(x, t)$.

Convergence to the Euler solution? Let us now compare the numerical solutions of the Leray system (3) to the Euler solution (41) when the smoothing parameter α decreases to 0. In Figure 2 we plot the entropic Euler solution (41) and the solution of the Leray system with $\alpha = 0.05$ at the final time $T = 3$. The numerical method uses a very fine spacetime grid with $N = 4001$ and $\Delta t = 0.0025$. Table 2 displays the relative L^2 -errors between the entropic Euler solution (41) and the numerical solutions of the Leray system with $\alpha = 0.4, 0.2, 0.1, 0.05$. The final time is $T = 3$, δ is fixed at 0.1 and the resolution used for all the runs is $N = 4001$ and $\Delta t = 0.0025$.

Table 2: Front-like initial data: convergence to the Euler solution? The table displays the relative L^2 -errors between the entropic Euler solution (41) and the numerical solutions of the Leray system for $\alpha = 0.4, 0.2, 0.1, 0.05$ at $T = 3$. For all the runs, $N = 4001$ and $\Delta t = 0.0025$. Note that the errors approach an $O(1)$ limit as α approaches 0.

	ρ : relative L^2 -error	v : relative L^2 -error
$\alpha = 0.4$	0.4530	9.4340×10^{-1}
$\alpha = 0.2$	0.4474	9.3453×10^{-1}
$\alpha = 0.1$	0.4470	9.3437×10^{-1}
$\alpha = 0.05$	0.4469	9.3435×10^{-1}

As Figure 2 shows, the solution computed using the Leray regularization has a shock that is clearly to the right of the shock in the exact entropy solution. This indicates that the Leray system fails to recover the correct shock speed. Also clearly shown in Figure 2 is that the Leray solutions $\rho(x, 3)$ and $v(x, 3)$ do match the exact solutions at the boundary, but the intermediate values ρ_{int} and v_{int} are wrong. The intermediate values for ρ and v are both noticeably larger than those of the exact solution.

We conclude that solutions of the Leray system (3) with smoothed Riemann initial data (38) do not, in the $\alpha \rightarrow 0$ limit, converge to a smoothed version of the exact entropy solution (41) of the Euler system (1).

Remark. We also performed a numerical study where the smoothing of the initial data is sequentially reduced, i.e. $\delta = 0.2, 0.1, 0.05$, and 0.025 , while keeping α fixed. We observed that

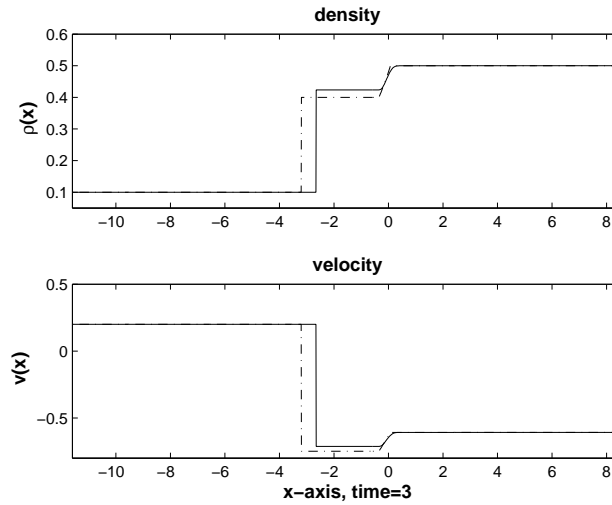


Figure 2: Front-like initial data. The solid line represents the numerical solution at $T = 3$ of the Leray system with $\alpha = 0.05$. The numerical calculation uses a very fine spacetime grid with $N = 4001$ and $\Delta t = 0.0025$. The dash-dot line represents the exact entropy solution of the Euler equations computed using (41). Note the order $O(1)$ error between the two solutions.

the shock location and the value of the jump at the shock remain unchanged. The only difference can be noted in the rarefaction fan which becomes steeper as δ decreases. This suggests that, besides failing to capture the correct shock speed and jump, the Leray regularization is also unable to recover the qualitative behavior of the rarefaction fan. As δ approaches 0, it seems that the Leray solutions converge to an unphysical shock, instead of a rarefaction fan, thus strengthening the conclusion of the present numerical study.

References

- [BaJG07] H. S. Bhat and R. C. Fetecau and J. Goodman, *A Leray-type regularization for the isentropic Euler equations*, *Nonlinearity* **20** (2007), 2035–2046.
- [BF06] H. S. Bhat and R. C. Fetecau, *A Hamiltonian regularization of the Burgers equation*, *J. Nonlinear Sci.* **16** (2006), no. 6, 615–638.
- [BF08] ———, *Stability of fronts for a regularization of the Burgers equation*, *Quart. Appl. Math.* **66** (2008), 473–496.
- [BF09] ———, *The Riemann problem for the Leray regularization of the Burgers equation*, *J. Differential Equations* (2009), in press.
- [CF76] R. Courant and K. O. Friedrichs, *Supersonic flow and shock waves*, Springer-Verlag, New York, 1976, Reprinting of the 1948 original, Applied Mathematical Sciences, Vol. 21.

- [Fol99] G. B. Folland, *Real analysis: modern techniques and their applications*, Wiley-Interscience, New York, 1999.
- [HK83] J. Hunter and J. B. Keller., *Weakly nonlinear high frequency waves*, Comm. Pure Appl. Math. **36** (1983), no. 5, 547–569.
- [HR02] H. Holden and N. H. Risebro, *Front tracking for hyperbolic conservation laws*, Applied Mathematical Sciences, vol. 152, Springer-Verlag, New York, 2002.
- [Ler34] J. Leray, *Essai sur le mouvement d'un fluide visqueux emplissant l'espace*, Acta Math. **63** (1934), 193–248.
- [MR84] A. Majda and R. Rosales, *Resonantly interacting weakly nonlinear hyperbolic waves. I. A single space variable*, Stud. Appl. Math. **71** (1984), no. 2, 149–179.
- [Smo83] J. Smoller, *Shock Waves and Reaction-Diffusion Equations*, Grundlehren der Mathematischen Wissenschaften, vol. 258, Springer-Verlag, New York, 1983.